Peer-to-peer Based Energy Management Framework for Enhancing Rural Electrification Level

Yi Liu, Xiao Xu, Chuanjiang Deng, Junyong Liu, Lixiong Xu, Youbo Liu, Nan Yang, Yichen Luo, and Shafqat Jawad

***Abstract*—Rural electrification is a crucial component of the power system that requires urgent innovation and transformation to enhance electrification levels. However, various challenges hinder the progress in rural electrification, primarily due to remote locations and unique consumption patterns. To effectively coordinate the local energy distribution, an energy management framework utilizing peer-to-peer (P2P) based interactive operations is proposed, which minimizes the reliance on long-distance transmission while enhancing the rural electrification level. The proposed P2P-based energy management framework incorporates various distributed generation resources across rural areas, facilitating direct energy transactions between neighboring community-based villages. Additionally, the P2P energy trading is modeled as a Nash bargaining (NB) problem, which accounts for the allocation of network loss costs and operational state of the rural distribution network. To protect the privacy of individual villages, an improved adaptive alternating direction method of multipliers (AADMM) is proposed to solve the NB problem. The AADMM utilizes a local curvature approximation scheme during parameter updates, allowing for automatic adjustments of the fixed penalty parameter within the standard alternating direction method of multipliers (ADMM). This enhancement improves the convergence rates without requiring central oversight. Simulation results demonstrate significant reductions in operational costs for both the overall network and individual village participants. The proposed P2P-based energy management framework also enhances the bus voltage stability and reduces the line transmission power, thereby further enhancing rural electrification levels. The adaptability and extensibility of this framework are further validated using the IEEE 33-bus and 118-bus distribution systems. Additionally, the AADMM shows higher convergence rates compared with the standard ADMM.**

***Index Terms*—Rural distribution network, peer-to-peer (P2P), energy trading, energy management, Nash bargaining, adaptive alternating direction method of multipliers (AADMM).**

I. Introduction

In recent decades, the rapid urbanization and rural-to-urban migration have emerged as global trends [1]. According to a World Bank survey, 56% of the world's population, or approximately 4.4 billion people, now reside in cities [2]. Despite the decreasing proportion of the rural population, a substantial number of individuals still reside in rural areas, many of whom lack access to electricity. This issue is particularly severe in many developing countries [3]. Rural electrification is essential for improving the life quality and stimulating the agricultural economy growth in these regions [4]. Thus, it is crucial to identify effective strategies for rural electrification.

A major factor leading to the slow development and persistent poverty in rural areas is the lack of electrification, as electricity is a prerequisite for various productive activities [5]. However, the electrification levels in these regions, particularly in many developing countries, remain insufficient to support the demands of the local economy and society, affecting transportation, education, income, infrastructure, living conditions [6], etc. Limited financial resources make it difficult for rural areas to afford the high costs of developing power infrastructure, thereby hindering the implementation of electrification projects [7]. Building transmission lines to supply electricity to remote and sparsely populated areas is often unattractive to investors, as the returns on such projects are insufficient to recover the investment costs [8]. Furthermore, the outdated and unreliable rural distribution systems pose significant challenges. These systems were originally designed with limited capacity, sufficient only for lighting and a few household appliances, and can not support large power demands. The construction of long-distance transmission lines in rural areas, combined with their limited capacity, also leads to voltage drop issues, adversely impacting power quality [9]. Additionally, the rural energy production often relies on traditional fossil fuels for power generation, and the high costs associated with coal, oil, and gas further impede the electrification. While rural areas possess

Manuscript received: April 19, 2024; revised: July 26, 2024; accepted: October 19, 2024. Date of CrossCheck: October 19, 2024. Date of online publication: November 28, 2024.

This work was supported by National Natural Science Foundation of China (No. 52207128).

Y. Liu, X. Xu (corresponding author), J. Liu, L. Xu, Y. Liu, Y. Luo, and S. Jawad are with the College of Electrical Engineering, Sichuan University, Chengdu, China (e-mail: liuy@stu.scu.edu.cn; xxiao@scu.edu.cn; liujy@scu.edu.cn; xulixiong@163. com; liuyoubo@scu. edu. cn; luoyc@stu. scu. edu. cn; engr.shafqatjawad@yahoo.com).

C. Deng is with the Aba Power Supply Company of State Grid Sichuan Electric Power Company, Abazhou Autonomous Prefecture, China (e-mail: 1278549072@qq.com).

N. Yang is with the College of Electrical Engineering and New Energy, China Three Gorges University, Yichang, China (e-mail: ynyyayy@ctgu.edu.cn).

DOI: 10.35833/MPCE.2024.000415

abundant resources and space for clean energy production, such as solar and wind power at lower costs, these opportunities remain largely underutilized. Another obstacle is the high electricity cost in rural areas, where there is usually only one provider, resulting in elevated prices due to a lack of competition.

As agricultural demands increase in remote rural areas, the distribution network from centralized power sources must be expanded to meet these needs. However, extending the centralized power system is economically unviable due to the significant mismatch between the low benefits derived from small load demands and the high costs of infrastructure [10]. Local distributed generation resources (DGRs) present an effective alternative by utilizing nearby power rather than extending the existing network [11]. Nevertheless, the current energy allocation mechanism leads to surplus energy and underutilization of resources. A community-based paradigm to sharing and trading energy among partners offers a viable solution for optimizing the power utilization and management in rural areas [12]. This peer-to-peer (P2P) energy trading enables community-based villages to sell excess electricity to other villages with higher demands. Additionally, villages can develop their own energy management infrastructure, reducing the need for extensive network expansion. This energy trading helps mitigate voltage drop issues and reduces transmission power. However, the research on the energy management framework and mechanisms in rural areas remains limited.

Recent research works on energy management in rural distribution networks (RDNs) have primarily focused on system operational strategies and output decisions of various energy units [13]-[16]. For instance, a new energy management algorithm is presented in [13], which adopts a mixed-integer linear programming model to ensure the optimal operating performance of an RDN. A distributionally robust day-ahead dispatch model for various energy devices is introduced in [14] to improve their utilization efficiencies. Additionally, an operational formulation developed in [15] considers multiple objectives based on economic and environmental factors for an RDN. Another study in [16] estimates the optimal design and operational strategies for a rural renewable system. These studies indeed demonstrate a centralized energy management framework for RDNs. Village participants are assumed to function as physical aggregators connected within the RDN, interacting with the upstream network. A virtual system operator dispatches energy from the upstream network to meet the energy demands of village participants and to maintain the operation of RDN. However, the centralized framework presents several crucial issues: ① it may incur higher costs due to long-distance energy transmission from a centralized source; and ② it emphasizes balancing power supply and demand in villages, which could result in wasted generation resources, such as excess wind and photovoltaic (PV) power. These challenges remain fundamental problems in recent energy management research on RDN and must be addressed. Therefore, this paper proposes an energy management framework for P2P-based interactive operations to tackle these challenges.

Several studies have investigated P2P energy trading using various models. In [17], the interaction between the distribution network service provider and multiple prosumers is modeled as a Stackelberg game, aiming to achieve the optimal network pricing and P2P energy trading simultaneously. Another study presents a three-stage multi-energy sharing strategy for a gas-electricity integrated energy system to address the multi-energy imbalance problem based on a P2P energy trading model [18]. A new dynamic operating envelope integrated with a P2P energy trading scheme is introduced in [19] to enhance the electricity exchange from prosumers to the distribution network. Additionally, a methodology based on the sensitivity analysis is proposed in [20] to evaluate the impact of P2P energy trading on the network. Various optimization models and methods based on P2P energy trading within distribution systems have also been developed in [21]-[23].

The optimization methods for P2P energy trading can be categorized into two main types: ① centralized optimization [24], [25]; and ② distributed optimization [26]-[28]. The centralized optimization methods face challenges related to computational costs and privacy concerns, primarily due to the necessity of sharing information among all peers. In contrast, the alternating direction method of multipliers (ADMM) is a well-known technique for the distributed optimization in P2P energy trading, providing enhanced privacy protection. Reference [29] proposes a distributed optimization method based on standard ADMM to develop the joint energy trading and scheduling strategies for multi-microgrids. Reference [30] employs the standard ADMM within microgrids, utilizing a two-phase approach to establish electricity operation strategies and determine the amount of energy traded. However, the performance of standard ADMM in optimizing P2P energy trading is poor, particularly in ill-conditioned or high-accuracy-required optimization problems. Additionally, the standard ADMM can require substantial computational time due to the extensive communication needed during each iteration. Therefore, it is crucial to enhance the convergence performance of standard ADMM for alleviating the computational burden and reduce the processing time.

The variants of the standard ADMM are very improtant to improve the performance. For example, a distributed consensus-based ADMM approach is proposed in [31] to address the optimal economic dispatch problems for multi-microgrids. Another study introduces a novel online consensus ADMM to maximize the social welfare and enable real-time P2P markets [32]. Additionally, an $l(p)$-box ADMM method is developed in [33] for the relaxation of binary variables in P2P energy trading. Another variant of ADMM is also implemented to improve the convergence rates, as detailed in [34]. These variants have demonstrated enhanced convergence performance across various studies. However, both the standard ADMM and its variants require a fixed penalty parameter across all iterations. The performance of ADMM is highly sensitive to the selection of the penalty parameter, often necessitating manual adjustments to suit different optimization problems and computational goals. An inappropriate penalty parameter can lead to slower convergence rate, increased computational time, and even failure to converge. Consequently, implementing an adaptive penalty parameter within ADMM offers a promising solution to improving the convergence performance and eliminating the need for manual tuning.

Several studies have explored suitable techniques for tuning the penalty parameter values at each iteration [35]-[39]. While various adaptive methods have been proposed [35]-[37], these adaptive ADMMs (AADMMs) are tailored to solve specific problems. For instance, [35] addresses the consensus-based optimization, [36] focuses on primal-dual hybrid gradient problems, and [37] deals with regularized estimation issues. Residual balancing (RB), discussed in [38], is a method that adjusts the penalty parameter in ADMM by balancing the primal and dual residuals. It seeks to keep both residuals at comparable magnitudes to adaptively adjust the penalty parameter. However, the performance of RB can vary significantly across different problem scales, potentially leading to convergence issues in ADMM for large-scale problems. Moreover, if the initial value of penalty parameter is inappropriate, its adaptation may occur slowly.

Based on the analysis, a comprehensive comparison of the existing literature is summarized as follows.

1) Lack of effective solutions to enhancing the rural electrification level. The development of rural power systems remains constrained by financial limitations. High capital costs related to the construction of long-distance transmission lines, outdated and unreliable rural distribution systems, limited transmission capacity, voltage drops, elevated electricity costs, and inadequate utilization of renewable energy sources all hinder improvements in electrification.

2) Lack of P2P-based energy management and market trading mechanisms. Some existing literature primarily emphasizes the centralized energy management, where rural community participants interact solely with the upstream grid. This leads to higher network loss costs and wasted renewable energy. The centralized energy management fails to address the challenges faced by the current rural power grid and may impede advancements in electrification levels.

3) Lack of efficient solution methods for P2P-based energy management and trading. The traditional ADMM requires manual tuning of initial penalty parameters to accommodate different problem scales, leading to high computational costs. While certain methods can adaptively adjust the penalty parameters, their performances remain inconsistent across various problem types.

These motivations and research gaps drive us to introduce a P2P-based energy management framework based on an improved ADMM-based distribution method, i. e., AADMM. This framework is designed to improve the local energy distribution and electrification levels in rural power systems. The contributions of this paper are as follows.

1) Proposing a P2P-based energy management framework for multiple rural community-based villages to enhance rural electrification levels. This framework employs the P2P energy trading to manage various local generation sources, with direct energy exchanges calculated by minimizing operational costs for both the RDN and villages.

2) Formulating the P2P energy trading among village participants as a Nash bargaining (NB) problem, considering the allocation of network loss costs. The NB problem is decomposed into two subproblems to effectively address its nonconvexity.

3) Introducing an improved ADMM-based distributed optimization method, i.e., AADMM, to tackle the P2P-based energy management framework. This method incorporates a local curvature approximation scheme during parameter update steps, enabling automatic tuning of the penalty parameter of the standard ADMM and improving the convergence performance.

The overall system model of the proposed P2P-based energy management framework, encompassing various components in villages and the operation model of RDN, is detailed in Section II. Section III presents the NB problem related to P2P energy trading, along with its two decomposed subproblems. The improved ADMM-based distributed optimization method, i. e., AADMM, is introduced in Section IV. Simulation results are provided in Section V. The conclusion is given in Section VI.

II. Proposed P2P-based Energy Management Framework

The proposed P2P-based energy management framework encompasses the RDN and various village participants. Models for the RDN and village participants are developed considering individual objectives, capability constraints, and technical limitations to facilitate the local optimization. Subsequently, the P2P energy trading model coordinates the optimization operations among the villages.

Figure 1 illustrates the energy and information connections in the proposed P2P-based energy management framework.

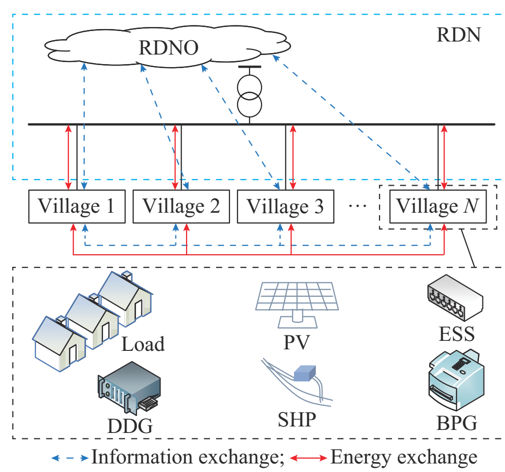

Fig. 1. Energy and information connections in proposed P2P-based energy management framework.

The community-based village participants integrate their DGRs to function as aggregators, located at various buses in the RDN. The DGRs include PV, diesel distributed generators (DDGs), energy storage systems (ESSs), small hydropower (SHP), and biomass power generators (BPGs) [40].

Village participants can purchase energy from or sell it to the upstream network at prices set by the RDN, and they can trade energy bilaterally at negotiated prices. A virtual rural distribution network operator (RDNO) provides a transparent platform for P2P energy trading without a physical entity, primarily focusing on tasks such as calculating trading power, prices, and scheduling releases. This paper assumes that village participants bear the network loss costs incurred from P2P energy trading. The role of RDNO is to minimize the total network loss costs and allocate these costs proportionally among the village participants.

A. Operation Model of Village Participants

1) Objective Function

In the proposed P2P-based energy management framework, village participants minimize the operational costs by scheduling various DGRs, including PV, DDG, ESS, SHP, and BPG. The total operational cost C_v for village participant v over the operational horizon $\mathbb{T}$ can be calculated using (1a). Note that not all villages may possess all these components. This paper assumes that PV incurs negligible marginal costs in the short run [29].

$$C_v=\sum_{t\in\mathbb{T}}(C_{v,\mathrm{DDG}}(t)+C_{v,\mathrm{SHP}}(t)+C_{v,\mathrm{BPG}}(t)+C_{v,\mathrm{ESS}}(t)+C_{v,\mathrm{Grid}}(t)) \tag{1a}$$

$$\begin{cases}C_{v,\mathrm{DDG}}(t)=a_2P_{v,\mathrm{DDG}}^2(t)+a_1P_{v,\mathrm{DDG}}(t)+a_0\\ C_{v,\mathrm{SHP}}(t)=b_{\mathrm{SHP}}P_{v,\mathrm{SHP}}(t)\\ C_{v,\mathrm{BPG}}(t)=c_{\mathrm{BPG}}P_{v,\mathrm{BPG}}(t)\\ C_{v,\mathrm{ESS}}(t)=d_{\mathrm{ESS}}(P_{v,\mathrm{ESS}}^{\mathrm{char}}(t)+P_{v,\mathrm{ESS}}^{\mathrm{disc}}(t))\\ C_{v,\mathrm{Grid}}(t)=e_{\mathrm{Grid}}^{\mathrm{p}}P_{v,\mathrm{Grid}}^{\mathrm{p}}(t)-e_{\mathrm{Grid}}^{\mathrm{s}}P_{v,\mathrm{Grid}}^{\mathrm{s}}(t)\end{cases} \tag{1b}$$

where $\mathbb{T}=\{1,2,\ldots t,\ldots,T\}$; $v\in\mathbb{V}$ are the index and set of villages participating in the P2P energy trading, respectively; $C_{v,\mathrm{DDG}}(t)$, $C_{v,\mathrm{SHP}}(t)$, $C_{v,\mathrm{BPG}}(t)$, and $C_{v,\mathrm{ESS}}(t)$ are the operational costs of DDG, SHP, BPG, and ESS in village v, respectively; $C_{v,\mathrm{Grid}}(t)$ is the energy exchange between village v and the upstream network; $P_{v,\mathrm{DDG}}(t)$, $P_{v,\mathrm{SHP}}(t)$, and $P_{v,\mathrm{BPG}}(t)$ are the output power of DDG, SHP, and BPG in village v, respectively; $P_{v,\mathrm{ESS}}^{\mathrm{char}}(t)$ and $P_{v,\mathrm{ESS}}^{\mathrm{disc}}(t)$ are the charging and discharging power of ESS in village v, respectively; $P_{v,\mathrm{Grid}}^{\mathrm{p}}(t)$ and $P_{v,\mathrm{Grid}}^{\mathrm{s}}(t)$ are the importing and exporting power with the upstream network, respectively; a_0, a_1, and a_2 are the generation cost coefficients for DDG; and b_{SHP}, c_{BPG}, d_{ESS}, $e_{\mathrm{Grid}}^{\mathrm{p}}$, and $e_{\mathrm{Grid}}^{\mathrm{s}}$ are the unit costs for SHP generation, BPG generation, ESS charging/discharging, purchasing energy from the upstream network, and selling energy to the upstream network, respectively.

2) Constraints

The output power of PV system in village v $P_{v,\mathrm{PV}}(t)$ should be constrained by:

$$P_{v,\mathrm{PV}}^{\min}\le P_{v,\mathrm{PV}}(t)\le P_{v,\mathrm{PV}}^{\max} \tag{2}$$

where $P_{v,\mathrm{PV}}^{\min}$ and $P_{v,\mathrm{PV}}^{\max}$ are the minimum and maximum output power of PV system in village v, respectively.

The output power of DDG should be subject to the following constraint:

$$P_{v,\mathrm{DDG}}^{\min}\le P_{v,\mathrm{DDG}}(t)\le P_{v,\mathrm{DDG}}^{\max} \tag{3}$$

where $P_{v,\mathrm{DDG}}^{\min}$ and $P_{v,\mathrm{DDG}}^{\max}$ are the minimum and maximum output power of DDG in village v, respectively.

The operational limitations of ESS are described as:

$$\begin{cases}0\le P_{v,\mathrm{ESS}}^{\mathrm{char}}(t)\le P_{v,\mathrm{ESS}}^{\mathrm{char,max}}x_{\mathrm{ESS}}^{\mathrm{char}}(t)\\ 0\le P_{v,\mathrm{ESS}}^{\mathrm{disc}}(t)\le P_{v,\mathrm{ESS}}^{\mathrm{disc,max}}x_{\mathrm{ESS}}^{\mathrm{disc}}(t)\\ 0\le x_{\mathrm{ESS}}^{\mathrm{char}}(t)+x_{\mathrm{ESS}}^{\mathrm{disc}}(t)\le 1\\ E_v(t+1)=E_v(t)+\left(\mu_{v,\mathrm{char}}P_{v,\mathrm{ESS}}^{\mathrm{char}}(t)-\dfrac{1}{\mu_{v,\mathrm{disc}}}P_{v,\mathrm{ESS}}^{\mathrm{disc}}(t)\right)\\ SoC_v^{\min}\le E_v(t)/E_v^{\max}\le SoC_v^{\max}\end{cases} \tag{4}$$

where $P_{v,\mathrm{ESS}}^{\mathrm{char,max}}$ and $P_{v,\mathrm{ESS}}^{\mathrm{disc,max}}$ are the maximum charging and discharging power of ESS in village v, respectively; $\mu_{v,\mathrm{char}}$ and $\mu_{v,\mathrm{disc}}$ are the charging and discharging efficiencies of ESS, respectively; $SoC_v^{\min}$ and $SoC_v^{\max}$ are the minimum and maximum states of charge (SoCs) of battery in village v, respectively; $E_v^{\max}$ is the maximum energy capacity of battery in village v; and $x_{\mathrm{ESS}}^{\mathrm{char}}(t)$ and $x_{\mathrm{ESS}}^{\mathrm{disc}}(t)$ are two binary variables for ESS charging and discharging, respectively. $x_{\mathrm{ESS}}^{\mathrm{char}}(t)=1$ when the ESS is charging, and $x_{\mathrm{ESS}}^{\mathrm{disc}}(t)=1$ when it is discharging; otherwise, $x_{\mathrm{ESS}}^{\mathrm{char}}(t)=0$ and $x_{\mathrm{ESS}}^{\mathrm{disc}}(t)=0$. The expression in the third line of constraint (4) prevents the simultaneous charging and discharging of ESS.

The output limitation of SHP can be described as:

$$P_{v,\mathrm{SHP}}^{\min}\le P_{v,\mathrm{SHP}}(t)\le P_{v,\mathrm{SHP}}^{\max} \tag{5}$$

where $P_{v,\mathrm{SHP}}^{\min}$ and $P_{v,\mathrm{SHP}}^{\max}$ are the minimum and maximum output power of SHP in village v, respectively.

The output power of BPG should be bounded by:

$$P_{v,\mathrm{BPG}}^{\min}\le P_{v,\mathrm{BPG}}(t)\le P_{v,\mathrm{BPG}}^{\max} \tag{6}$$

where $P_{v,\mathrm{BPG}}^{\min}$ and $P_{v,\mathrm{BPG}}^{\max}$ are the minimum and maximum output power of BPG in village v, respectively.

The exchange power between village participants and the upstream network must be constrained within specific limits as:

$$\begin{cases}0\le P_{v,\mathrm{Grid}}^{\mathrm{p}}(t)\le P_{v,\mathrm{Grid}}^{\mathrm{p,max}}\\ 0\le P_{v,\mathrm{Grid}}^{\mathrm{s}}(t)\le P_{v,\mathrm{Grid}}^{\mathrm{s,max}}\end{cases} \tag{7}$$

where $P_{v,\mathrm{Grid}}^{\mathrm{p,max}}$ and $P_{v,\mathrm{Grid}}^{\mathrm{s,max}}$ are the maximum purchasing and selling power of village v, respectively.

Additionally, village v must maintain an active power balance during time slot t, as described in (8).

$$\begin{aligned}&P_{v,\mathrm{PV}}(t)+P_{v,\mathrm{DDG}}(t)+P_{v,\mathrm{SHP}}(t)+P_{v,\mathrm{BPG}}(t)+P_{v,\mathrm{ESS}}^{\mathrm{disc}}(t)+\\ &P_{v,\mathrm{Grid}}^{\mathrm{p}}(t)=P_{v,\mathrm{L}}(t)+P_{v,\mathrm{ESS}}^{\mathrm{char}}(t)+P_{v,\mathrm{Grid}}^{\mathrm{s}}(t)\end{aligned} \tag{8}$$

where $P_{v,\mathrm{L}}(t)$ is the energy demand of village v.

B. Operation Model of RDN

1) Objective Function

Considering the radial network in rural areas, the DistFlow model is used to calculate the power flow and network losses in this work [41]. Let $\mathbb{G}=(\mathbb{B},\mathbb{E})$ denote the radial topology of the RDN, where $\mathbb{B}$ and $\mathbb{E}$ are the sets of buses and branches, respectively. Let $0\in\mathbb{B}$ denote the slack bus in set $\mathbb{G}$, through which the upstream network is connected as an external power source for RDN. The network loss is non-negligible due to the high R/X ratio. The objective function (9) calculates the total network loss cost C_{loss} as:

$$C_{\mathrm{loss}}=c_{\mathrm{loss}}\sum_{t\in\mathbb{T}}\sum_{(i,j)\in\mathbb{E}}r_{ij}l_{ij}(t) \tag{9}$$

where c_{loss} is the per-unit network loss cost; r_{ij} is the resistance of branch $(i,j)\in\mathbb{E}$; and $l_{ij}(t)=\left|I_{ij}(t)\right|^2$, and $I_{ij}(t)$ is the current from buses i to j.

2) Constraints

The operational constraints of RDN are presented as:

$$\begin{cases} p_j(t)=P_{ij}(t)-r_{ij}l_{ij}(t)-\sum\limits_{k\neq i:(j,k)}P_{jk}(t)\\ q_j(t)=Q_{ij}(t)-x_{ij}l_{ij}(t)-\sum\limits_{k\neq i:(j,k)}Q_{jk}(t)\end{cases} \tag{10a}$$

$$v_j(t)=v_i(t)-2(r_{ij}P_{ij}(t)+x_{ij}Q_{ij}(t))+(r_{ij}^2+x_{ij}^2)l_{ij}(t) \tag{10b}$$

$$l_{ij}(t)=(P_{ij}^2(t)+Q_{ij}^2(t))/v_i(t) \tag{10c}$$

$$P_{ij}(t)\leq P_{ij}^{\max}(t) \tag{10d}$$

$$Q_{ij}(t)\leq Q_{ij}^{\max}(t) \tag{10e}$$

$$V_i^{\min}(t)\leq V_i(t)\leq V_i^{\max}(t) \tag{10f}$$

$$l_{ij}(t)\geq(P_{ij}^2(t)+Q_{ij}^2(t))/v_i(t) \tag{10g}$$

where $p_j(t)$ and $q_j(t)$ are the active and reactive power injections at bus $j\in\mathbb{B}$, respectively; $P_{ij}(t)$ and $Q_{ij}(t)$ are the active and reactive power flows of branch $(i,j)\in\mathbb{E}$, respectively; $\sum\limits_{k\neq i:(j,k)}P_{jk}(t)$ and $\sum\limits_{k\neq i:(j,k)}Q_{jk}(t)$ are the sums of the active and reactive power flows of all branches connected to bus j excluding branch (i,j), respectively; x_{ij} is the reactance of branch $(i,j)\in\mathbb{E}$; $v_i(t)=\left|V_i(t)\right|^2$, with $V_i(t)$ being the voltage magnitude of bus i; $V_i^{\min}(t)$ and $V_i^{\max}(t)$ are the minimum and maximum voltage magnitudes of bus i, respectively; and $P_{ij}^{\max}(t)$ and $Q_{ij}^{\max}(t)$ are the maximum active and reactive power flows of branch $(i,j)\in\mathbb{E}$, respectively. Given the issue of nonconvexity, constraint (10c) is reformulated using second-order cone programming relaxation as (10g).

C. P2P Energy Trading Model

Village participants engage in the P2P energy trading with neighboring villages, negotiating the amount and price of exchangeable energy bilaterally. The energy exchanged between villages m and n, along with their net importing and exporting power, represented by $e_m^+(t)$ and $e_n^-(t)$, respectively, can be defined as:

$$e_m^+(t)=\sum_{n\in\mathbb{V}^-}e_{m,n}^+(t) \tag{11a}$$

$$e_n^-(t)=\sum_{m\in\mathbb{V}^+}e_{n,m}^-(t) \tag{11b}$$

$$e_{m,n}^+(t)=e_{n,m}^-(t) \tag{11c}$$

where $m\in\mathbb{V}^+$ and $n\in\mathbb{V}^-$ are the indices of villages participating in P2P energy trading as energy purchasers and sellers, respectively, and $\mathbb{V}^+\bigcup\mathbb{V}^-=\mathbb{V}$; and $e_{m,n}^+(t)$ and $e_{n,m}^-(t)$ are the importing and exporting power of villages $m\in\mathbb{V}^+$ and $n\in\mathbb{V}^+$, respectively.

The power balance constraint (8) can be rewritten as (12) for villages $m\in\mathbb{V}^+$ and $n\in\mathbb{V}^-$.

$$\begin{cases} P_{v,\mathrm{PV}}(t)+P_{v,\mathrm{DDG}}(t)+P_{v,\mathrm{SHP}}(t)+P_{v,\mathrm{BPG}}(t)+P_{v,\mathrm{ESS}}^{\mathrm{disc}}(t)+\\ \qquad P_{v,\mathrm{Grid}}^{\mathrm{p}}(t)+e_m^+(t)=P_{v,\mathrm{L}}(t)+P_{v,\mathrm{ESS}}^{\mathrm{char}}(t)+P_{v,\mathrm{Grid}}^{\mathrm{s}}(t)\\ P_{v,\mathrm{PV}}(t)+P_{v,\mathrm{DDG}}(t)+P_{v,\mathrm{SHP}}(t)+P_{v,\mathrm{BPG}}(t)+P_{v,\mathrm{ESS}}^{\mathrm{disc}}(t)+\\ \qquad P_{v,\mathrm{Grid}}^{\mathrm{p}}(t)=P_{v,\mathrm{L}}(t)+P_{v,\mathrm{ESS}}^{\mathrm{char}}(t)+P_{v,\mathrm{Grid}}^{\mathrm{s}}(t)+e_n^-(t)\end{cases} \tag{12}$$

III. NB Problem for Proposed P2P-based Energy Management Framework

Direct energy trading among villages can effectively increase profits and reduce operational costs. However, the unfair profit allocation may diminish the willingness of villages to participate in P2P energy trading. As a crucial component of cooperative game theory, the NB solution can manage the complex interests among agents in a multi-agent energy system. It provides a Pareto optimal solution that balances individual interests and achieves a fair benefit allocation scheme. Consequently, the proposed P2P-based energy management framework formulates the energy trading process as an NB problem to incentivize direct energy trading among villages.

A typical NB problem is modeled as:

$$\begin{cases} \max\ \prod\limits_{s=1}^{S}(U_s-U_s^0)\\ \text{s.t. } U_s\geq U_s^0\end{cases} \tag{13}$$

where S is the number of bargaining players; U_s is the benefit of player s; and U_s^0 is the disagreement point.

This disagreement point signifies the situation where bargaining players fail to cooperate, potentially due to issues such as unfair benefit allocation. Accordingly, U_s^0 indicates the benefit of player s when the cooperation breaks down due to negotiation failure.

Model (13) is a non-convex nonlinear optimization model, the complexity of which increases due to the constraints involved. To ensure the computational tractability, the NB problem is decomposed into two manageable subproblems: the operational cost minimization problem and the energy trading payment problem. The two subproblems are solved sequentially to determine the optimal energy trading schemes for the villages.

Villages $m\in\mathbb{V}^+$ and $n\in\mathbb{V}^-$ are willing to participate in P2P energy trading only if the following constraints are satisfied.

$$C_m^++C_{m,\mathrm{loss}}^++\pi_m^+\leq C_m^{\mathrm{non}} \tag{14a}$$

$$C_n^-+C_{n,\mathrm{loss}}^-+\pi_n^-\leq C_n^{\mathrm{non}} \tag{14b}$$

$$C_m^{\mathrm{non}}=\sum_{t\in\mathbb{T}}(C_{m,\mathrm{DDG}}^{\mathrm{non}}(t)+C_{m,\mathrm{SHP}}^{\mathrm{non}}(t)+C_{m,\mathrm{BPG}}^{\mathrm{non}}(t)+C_{m,\mathrm{ESS}}^{\mathrm{non}}(t)+C_{m,\mathrm{Grid}}^{\mathrm{non}}(t)) \tag{14c}$$

$$C_n^{\mathrm{non}}=\sum_{t\in\mathbb{T}}(C_{n,\mathrm{DDG}}^{\mathrm{non}}(t)+C_{n,\mathrm{SHP}}^{\mathrm{non}}(t)+C_{n,\mathrm{BPG}}^{\mathrm{non}}(t)+C_{n,\mathrm{ESS}}^{\mathrm{non}}(t)+C_{n,\mathrm{Grid}}^{\mathrm{non}}(t)) \tag{14d}$$

where C_m^+ and C_n^- are the internal operational costs for villages $m\in\mathbb{V}^+$ and $n\in\mathbb{V}^-$ participating in P2P energy trading, respectively, as defined in (1); C_m^{non} and C_n^{non} are the operational costs for villages $m\in\mathbb{V}^+$ and $n\in\mathbb{V}^-$ without participating in P2P energy trading, which are also calculated based on objective (1), as described in (14c) and (14d), respectively; π_m^+ and π_n^- are the P2P energy trading payments for villages $m \in \mathbb{V}^+$ and $n \in \mathbb{V}^-$, respectively, which are the costs associated with power exchange; and $C_{m,\text{loss}}^+$ and $C_{n,\text{loss}}^-$ are the network loss costs imposed on villages $m \in \mathbb{V}^+$ and $n \in \mathbb{V}^-$, respectively.

In this paper, the total network loss cost is proportionally allocated to villages participating in the P2P energy trading based on their exchanged power. Therefore, $C_{m,\text{loss}}^+$ and $C_{n,\text{loss}}^-$ are defined based on objective (9) as:

$$C_{m,\text{loss}}^+ = \frac{e_m^+(t)}{\sum\limits_{m \in \mathbb{V}^+} e_m^+(t) + \sum\limits_{n \in \mathbb{V}^-} e_n^-(t)} C_{\text{loss}} \tag{15a}$$

$$C_{n,\text{loss}}^- = \frac{e_n^-(t)}{\sum\limits_{m \in \mathbb{V}^+} e_m^+(t) + \sum\limits_{n \in \mathbb{V}^-} e_n^-(t)} C_{\text{loss}} \tag{15b}$$

The P2P energy trading payments π_m^+ and π_n^- are subject to:

$$\sum_{m \in \mathbb{V}^+} \pi_m^+ + \sum_{n \in \mathbb{V}^-} \pi_n^- = 0 \tag{16}$$

Notably, it can be observed that C_m^{non} and C_n^{non} in (14) correspond to U_s^0 in (13). Similarly, $C_m^+ + C_{m,\text{loss}}^+ + \pi_m^+$ and $C_n^- + C_{n,\text{loss}}^- + \pi_n^-$ in (14) correspond to U_s in (13). The symbol ≥ in (13) changes to ≤ in (14) because the former represents benefits while the latter represents costs. Hence, the NB problem of P2P energy trading within the proposed P2P-based energy management framework is described by incorporating (14) and (15) into (13) as:

$$\begin{cases} \max\limits_{\{\mathbb{M}_m^+, \mathbb{P}_m^+, \mathbb{M}_n^-, \mathbb{P}_n^-, \mathbb{M}_{\text{RDN}}\}} \left\{ \prod\limits_{m \in \mathbb{V}^+} (C_m^{\text{non}} - C_m^+ - C_{m,\text{loss}}^+ - \pi_m^+) \cdot \right. \\ \left. \qquad \prod\limits_{n \in \mathbb{V}^-} (C_n^{\text{non}} - C_n^- - C_{n,\text{loss}}^- - \pi_n^-) \right\} \\ \text{s.t. } (2)\text{-}(7),\ (10)\text{-}(12),\ (16) \end{cases} \tag{17a}$$

$$\mathbb{M}_m^+ = \mathbb{M}_n^- := \{P_{v,\text{PV}}(t), P_{v,\text{DDG}}(t), P_{v,\text{SHP}}(t), P_{v,\text{BPG}}(t), P_{v,\text{ESS}}^{\text{char}}(t), P_{v,\text{ESS}}^{\text{disc}}(t)\} \tag{17b}$$

$$\mathbb{P}_m^+ := \{P_{m,\text{Grid}}^{\text{p}+}(t), P_{m,\text{Grid}}^{\text{s}+}(t), e_m^+(t)\} \tag{17c}$$

$$\mathbb{P}_n^- := \{P_{m,\text{Grid}}^{\text{p}-}(t), P_{n,\text{Grid}}^{\text{s}-}(t), e_n^-(t)\} \tag{17d}$$

$$\mathbb{M}_{\text{RDN}} := \{p_j(t), q_j(t), P_{ij}(t), Q_{ij}(t), v_i(t), l_{ij}(t)\} \tag{17e}$$

where $\mathbb{M}_m^+$ and $\mathbb{M}_n^-$ are the sets of decision variables for DGRs within villages $m \in \mathbb{V}^+$ and $n \in \mathbb{V}^-$, respectively; $\mathbb{P}_m^+$ and $\mathbb{P}_n^-$ are the sets of decision variables for power imports and exports with the upstream network and through P2P energy trading, respectively; and $\mathbb{M}_{\text{RDN}}$ is the set of decision variables for RDN.

Objective (1) for P2P energy trading is represented by C_m^+ and C_n^- in the NB problem (17), while objective (9) is represented by $C_{m,\text{loss}}^+$ and $C_{n,\text{loss}}^-$.

The NB problem (17) can be decomposed into two subproblems: the operational cost minimization problem of the RDN (P1) and the payment bargaining problem (P2), described as:

P1:

$$\begin{cases} \min\limits_{\{\mathbb{M}_m^+, \mathbb{P}_m^+, \mathbb{M}_n^-, \mathbb{P}_n^-, \mathbb{M}_{\text{RDN}}\}} \left\{ \sum\limits_{m \in \mathbb{V}^+} (C_m^+ + C_{m,\text{loss}}^+) + \sum\limits_{n \in \mathbb{V}^-} (C_n^- + C_{n,\text{loss}}^-) \right\} \\ \text{s.t. } (2)\text{-}(7),\ (10)\text{-}(12) \end{cases} \tag{18a}$$

P2:

$$\begin{cases} \max\limits_{\{\pi_m^+, \pi_n^-\}} \left\{ \prod\limits_{m \in \mathbb{V}^+} (C_m^{\text{non}} - C_{m*}^+ - C_{m,\text{loss}*}^+ - \pi_m^+) \cdot \right. \\ \left. \qquad \prod\limits_{n \in \mathbb{V}^-} (C_n^{\text{non}} - C_{n*}^- - C_{n,\text{loss}*}^- - \pi_n^-) \right\} \\ \text{s.t. } (14)\text{-}(16) \end{cases} \tag{18b}$$

where C_{m*}^+, C_{n*}^-, $C_{m,\text{loss}*}^+$, and $C_{n,\text{loss}*}^-$ are the optimal solutions in P1.

The process for jointly solving P1 and P2 is divided into several steps, as shown in Supplementary Material A Fig. SA1.

IV. Improved ADMM-based Distributed Method

This section presents an improved ADMM-based distributed method, i.e., AADMM, to address the NB problem in the P2P energy trading. This method only leverages partial information from each participant to optimize trading schemes, thereby ensuring substantial protection of peer privacy. The AADMM decomposes the optimization problems into sequences of simpler subproblems, which enhances the computational efficiency. This is crucial for ensuring the algorithm convergence and reducing the computational time when tackling complex optimization problems. However, the standard ADMM typically employs a fixed penalty parameter, and its convergence performance is significantly influenced by the initial setting of this penalty parameter. This necessitates manual adjustment tailored to each optimization problem to determine the convergence speed. To address this challenge, the AADMM utilizes a local curvature approximation scheme to automatically adapt the penalty parameter, thus eliminating the need for manual oversight [42].

The form of standard ADMM can be formulated as:

$$\begin{cases} \min\limits_{\boldsymbol{u},\boldsymbol{v}} \{\boldsymbol{H}(\boldsymbol{u}) + \boldsymbol{G}(\boldsymbol{v})\} \\ \text{s.t. } \boldsymbol{A}\boldsymbol{u} + \boldsymbol{B}\boldsymbol{v} = \boldsymbol{b} \end{cases} \tag{19}$$

where $\boldsymbol{H}(\boldsymbol{u})$ and $\boldsymbol{G}(\boldsymbol{v})$ are the closed convex functions, and $\boldsymbol{u}$ and $\boldsymbol{v}$ are the variables of these two functions, respectively; $\boldsymbol{A}$ and $\boldsymbol{B}$ are the coefficients of variables $\boldsymbol{u}$ and $\boldsymbol{v}$ in the constraints, respectively; and $\boldsymbol{b}$ is the vector of constants in the constraints.

The augmented Lagrangian function is shown as:

$$\mathcal{L}(\boldsymbol{u},\boldsymbol{v},\boldsymbol{\lambda}) = \boldsymbol{H}(\boldsymbol{u}) + \boldsymbol{G}(\boldsymbol{v}) + \boldsymbol{\lambda}^{\mathrm{T}}(\boldsymbol{b} - \boldsymbol{A}\boldsymbol{u} - \boldsymbol{B}\boldsymbol{v}) + \frac{\rho}{2}\|\boldsymbol{b} - \boldsymbol{A}\boldsymbol{u} - \boldsymbol{B}\boldsymbol{v}\|_2^2 \tag{20}$$

where ρ is the penalty parameter; and $\boldsymbol{\lambda}$ is the Lagrangian multiplier, i.e., dual variable.

The values of $\boldsymbol{u}$, $\boldsymbol{v}$, and $\boldsymbol{\lambda}$ in iteration $k+1$ can be described as:

$$\boldsymbol{u}_{k+1}=\arg\min_{\boldsymbol{u}}\left\{\boldsymbol{H}(\boldsymbol{u})+\boldsymbol{\lambda}_k^{\mathrm{T}}(\boldsymbol{b}-\boldsymbol{A}\boldsymbol{u}-\boldsymbol{B}\boldsymbol{v}_k)+\frac{\rho}{2}\left\|\boldsymbol{b}-\boldsymbol{A}\boldsymbol{u}-\boldsymbol{B}\boldsymbol{v}_k\right\|_2^2\right\} \tag{21a}$$

$$\boldsymbol{v}_{k+1}=\arg\min_{\boldsymbol{v}}\left\{\boldsymbol{G}(\boldsymbol{v})+\boldsymbol{\lambda}_k^{\mathrm{T}}(\boldsymbol{b}-\boldsymbol{A}\boldsymbol{u}_{k+1}-\boldsymbol{B}\boldsymbol{v})+\frac{\rho}{2}\left\|\boldsymbol{b}-\boldsymbol{A}\boldsymbol{u}_{k+1}-\boldsymbol{B}\boldsymbol{v}\right\|_2^2\right\} \tag{21b}$$

$$\boldsymbol{\lambda}_{k+1}=\boldsymbol{\lambda}_k+\rho(\boldsymbol{b}-\boldsymbol{A}\boldsymbol{u}_{k+1}-\boldsymbol{B}\boldsymbol{v}_{k+1}) \tag{21c}$$

The primal residual $\boldsymbol{r}_k$ and dual residual $\boldsymbol{d}_k$ in iteration k are introduced as:

$$\begin{cases}\boldsymbol{r}_k=\boldsymbol{b}-\boldsymbol{A}\boldsymbol{u}_k-\boldsymbol{B}\boldsymbol{v}_k\\ \boldsymbol{d}_k=\rho\boldsymbol{A}^{\mathrm{T}}\boldsymbol{B}(\boldsymbol{v}_k-\boldsymbol{v}_{k-1})\end{cases} \tag{22}$$

The stopping criteria of standard ADMM is described as:

$$\varepsilon=\max\left\{\frac{\left\|\boldsymbol{r}_k\right\|_2}{\max\left\{\left\|\boldsymbol{A}\boldsymbol{u}_k\right\|_2,\left\|\boldsymbol{B}\boldsymbol{v}_k\right\|_2,\left\|\boldsymbol{b}\right\|_2\right\}},\frac{\left\|\boldsymbol{d}_k\right\|_2}{\left\|\boldsymbol{A}^{\mathrm{T}}\boldsymbol{\lambda}_k\right\|_2}\right\}\le\varepsilon^{tol} \tag{23}$$

where ε and ε^{tol} are the relative residual and stopping tolerances, respectively.

This paper leverages spectral gradient methods from [43] to improve the fixed penalty parameter in standard ADMM for accelerating convergence. The spectral gradient method, pioneered by Barzilai and Borwein as a variant of gradient descent, is referred to as the BB method. The mathematical formulation of traditional gradient descent method for optimizing an objective function F without constraints can be described as [44]:

$$x_{k+1}=x_k-\tau_k\nabla F(x_k) \tag{24}$$

where x and x_{k+1} are the decision variables for function F in iterations k and $k+1$, respectively; and τ_k is the step size in iteration k.

The BB method sets $\tau_k=\alpha_k$ and adaptively chooses the step size τ_k for rapid convergence, where α_k is a curvature estimate of the optimization objective F. The curvature estimate α_k can be calculated using a least squares criterion as:

$$\alpha_k=\arg\min_{\alpha}\left\|\nabla F(x_k)-\nabla F(x_{k-1})-\alpha(x_k-x_{k-1})\right\|_2^2 \tag{25}$$

Inspired by the BB method, the fixed penalty parameter ρ in standard ADMM is formulated by the curvature estimates of $\boldsymbol{H}(\cdot)$ and $\boldsymbol{G}(\cdot)$ in (19) to enable the adaptive adjustment. However, the BB method is primarily designed for solving unconstrained minimization problems. Hence, Douglas-Rachdord splitting (DRS) [45] is used to transform the constrained ADMM in (19) into its Fenchel dual, thereby converting it into an unconstrained minimization problem as described in (26). Further, the penalty parameter ρ is converted to the curvature estimates in (26). The dual form of (19) is given as:

$$\min_{\boldsymbol{\lambda}\in\mathbf{R}^{N_\lambda}}\left\{\underbrace{\boldsymbol{H}^*(\boldsymbol{A}^{\mathrm{T}}\boldsymbol{\lambda})-\boldsymbol{\lambda}^{\mathrm{T}}\boldsymbol{b}}_{\hat{\boldsymbol{H}}(\boldsymbol{\lambda})}+\underbrace{\boldsymbol{G}^*(\boldsymbol{B}^{\mathrm{T}}\boldsymbol{\lambda})}_{\hat{\boldsymbol{G}}(\boldsymbol{\lambda})}\right\} \tag{26}$$

where $\boldsymbol{H}^*(\cdot)$ and $\boldsymbol{G}^*(\cdot)$ are defined as the conjugate functions of $\boldsymbol{H}(\cdot)$ and $\boldsymbol{G}(\cdot)$, respectively; and $\hat{\boldsymbol{H}}(\cdot)$ and $\hat{\boldsymbol{G}}(\cdot)$ are the newly-defined functions.

A dual variable $\hat{\boldsymbol{\lambda}}_{k+1}$, distinct from standard ADMM, is defined as $\hat{\boldsymbol{\lambda}}_{k+1}=\boldsymbol{\lambda}_k+\tau_k(\boldsymbol{b}-\boldsymbol{A}\boldsymbol{u}_{k+1}-\boldsymbol{B}\boldsymbol{v}_k)$. The optimality conditions for (21a) and (21b) are formulated as:

$$\begin{cases}\partial\boldsymbol{H}(\boldsymbol{u}_{k+1})-\boldsymbol{A}^{\mathrm{T}}[\boldsymbol{\lambda}_k+\tau_k(\boldsymbol{b}-\boldsymbol{A}\boldsymbol{u}_{k+1}-\boldsymbol{B}\boldsymbol{v}_k)]=\boldsymbol{0}\\ \partial\boldsymbol{G}(\boldsymbol{v}_{k+1})-\boldsymbol{B}^{\mathrm{T}}[\boldsymbol{\lambda}_k+\tau_k(\boldsymbol{b}-\boldsymbol{A}\boldsymbol{u}_{k+1}-\boldsymbol{B}\boldsymbol{v}_{k+1})]=\boldsymbol{0}\end{cases} \tag{27}$$

The two equations in (27) are equivalent to $\partial\boldsymbol{H}(\boldsymbol{u}_{k+1})=\boldsymbol{A}^{\mathrm{T}}\hat{\boldsymbol{\lambda}}_{k+1}$ and $\partial\boldsymbol{G}(\boldsymbol{v}_{k+1})=\boldsymbol{B}^{\mathrm{T}}\boldsymbol{\lambda}_{k+1}$.

Let $\boldsymbol{u}_{k+1}=\partial\boldsymbol{H}^*(\boldsymbol{A}^{\mathrm{T}}\hat{\boldsymbol{\lambda}}_{k+1})$ and $\boldsymbol{v}_{k+1}=\partial\boldsymbol{G}^*(\boldsymbol{B}^{\mathrm{T}}\boldsymbol{\lambda}_{k+1})$ according to [46]. $\partial\hat{\boldsymbol{H}}(\hat{\boldsymbol{\lambda}}_{k+1})=\boldsymbol{A}\boldsymbol{u}_{k+1}-\boldsymbol{b}$ and $\partial\hat{\boldsymbol{G}}(\boldsymbol{\lambda}_{k+1})=\boldsymbol{B}\boldsymbol{v}_{k+1}$ can be calculated using (26). The curvatures of $\hat{\boldsymbol{H}}(\cdot)$ and $\hat{\boldsymbol{G}}(\cdot)$ from the previous iterations (the number of the previous iterations is defined as T_f) are estimated using the least squares criterion based on the typical BB method as:

$$\begin{cases}\min\limits_{\alpha}\left\|\Delta\hat{\boldsymbol{H}}_k-\alpha\Delta\hat{\boldsymbol{\lambda}}_k\right\|_2^2\\ \min\limits_{\beta}\left\|\Delta\hat{\boldsymbol{G}}_k-\beta\Delta\boldsymbol{\lambda}_k\right\|_2^2\end{cases} \tag{28}$$

$$\Delta\hat{\boldsymbol{\lambda}}_k=\hat{\boldsymbol{\lambda}}_k-\hat{\boldsymbol{\lambda}}_{k_0} \tag{29a}$$

$$\Delta\boldsymbol{\lambda}_k=\boldsymbol{\lambda}_k-\boldsymbol{\lambda}_{k_0} \tag{29b}$$

$$\Delta\hat{\boldsymbol{H}}_k=\partial\hat{\boldsymbol{H}}(\hat{\boldsymbol{\lambda}}_k)-\partial\hat{\boldsymbol{H}}(\hat{\boldsymbol{\lambda}}_{k_0})=\boldsymbol{A}(\boldsymbol{u}_k-\boldsymbol{u}_{k_0}) \tag{29c}$$

$$\Delta\hat{\boldsymbol{G}}_k=\partial\hat{\boldsymbol{G}}(\boldsymbol{\lambda}_k)-\partial\hat{\boldsymbol{G}}(\boldsymbol{\lambda}_{k_0})=\boldsymbol{B}(\boldsymbol{v}_k-\boldsymbol{v}_{k_0}) \tag{29d}$$

where $k_0=k-T_f$ represents a prior iteration; and α and β are the curvatures formulated as:

$$\begin{cases}\alpha_k^{SD}=\dfrac{\left\langle\Delta\hat{\boldsymbol{\lambda}}_k,\Delta\hat{\boldsymbol{\lambda}}_k\right\rangle}{\left\langle\Delta\hat{\boldsymbol{H}}_k,\Delta\hat{\boldsymbol{\lambda}}_k\right\rangle}\\ \alpha_k^{MG}=\dfrac{\left\langle\Delta\hat{\boldsymbol{H}}_k,\Delta\hat{\boldsymbol{\lambda}}_k\right\rangle}{\left\langle\Delta\hat{\boldsymbol{H}}_k,\Delta\hat{\boldsymbol{H}}_k\right\rangle}\end{cases} \tag{30a}$$

$$\begin{cases}\beta_k^{SD}=\dfrac{\left\langle\Delta\boldsymbol{\lambda}_k,\Delta\boldsymbol{\lambda}_k\right\rangle}{\left\langle\Delta\hat{\boldsymbol{G}}_k,\Delta\boldsymbol{\lambda}_k\right\rangle}\\ \beta_k^{MG}=\dfrac{\left\langle\Delta\hat{\boldsymbol{G}}_k,\Delta\boldsymbol{\lambda}_k\right\rangle}{\left\langle\Delta\hat{\boldsymbol{G}}_k,\Delta\hat{\boldsymbol{G}}_k\right\rangle}\end{cases} \tag{30b}$$

where the superscripts SD and MG are the steepest descent and minimum gradient, respectively [47].

The hybrid step size rule, as stated in [47], is given as:

$$\alpha_k=\begin{cases}\alpha_k^{MG} & 2\alpha_k^{MG}>\alpha_k^{SD}\\ \alpha_k^{SD}-\dfrac{\alpha_k^{MG}}{2} & \text{otherwise}\end{cases} \tag{31a}$$

$$\beta_k=\begin{cases}\beta_k^{MG} & 2\beta_k^{MG}>\beta_k^{SD}\\ \beta_k^{SD}-\dfrac{\beta_k^{MG}}{2} & \text{otherwise}\end{cases} \tag{31b}$$

Further, the step size τ_k is calculated by $\sqrt{\alpha_k\beta_k}$.

Even with the improvements and refinements that enhance the computational efficiency of standard ADMM, the variations in step size can lead to unreliable curvature estimates. Consequently, the AADMM proposes a safeguarded method for reassessing curvature estimates, which is described as:

$$\tau_{k+1}=\begin{cases}\sqrt{\alpha_k\beta_k} & \alpha_k^{cor}>\varepsilon^{cor},\ \beta_k^{cor}>\varepsilon^{cor}\\ \alpha_k & \alpha_k^{cor}>\varepsilon^{cor},\ \beta_k^{cor}\le\varepsilon^{cor}\\ \beta_k & \alpha_k^{cor}\le\varepsilon^{cor},\ \beta_k^{cor}>\varepsilon^{cor}\\ \tau_k & \text{otherwise}\end{cases} \tag{32}$$

where ε^{cor} is the correlation threshold; and α_k^{cor} and β_k^{cor} are the correlations between $\Delta\hat{\boldsymbol{H}}_k$ and $\Delta\hat{\boldsymbol{\lambda}}_k$ and between $\Delta\hat{\boldsymbol{G}}_k$ and $\Delta\boldsymbol{\lambda}_k$, respectively, which are used to assess the reliability of curvature estimates and expressed as:

$$\begin{cases}\alpha_k^{cor}=\dfrac{\left\langle\Delta\hat{\boldsymbol{H}}_k,\Delta\hat{\boldsymbol{\lambda}}_k\right\rangle}{\left\|\Delta\hat{\boldsymbol{H}}_k\right\|\left\|\Delta\hat{\boldsymbol{\lambda}}_k\right\|}\\ \beta_k^{cor}=\dfrac{\left\langle\Delta\hat{\boldsymbol{G}}_k,\Delta\boldsymbol{\lambda}_k\right\rangle}{\left\|\Delta\hat{\boldsymbol{G}}_k\right\|\left\|\Delta\boldsymbol{\lambda}_k\right\|}\end{cases} \tag{33}$$

The generalized model of AADMM in (19)-(33) is derived through mathematical transformations from the standard ADMM. The key parameters in the AADMM, including curvatures α_k and β_k, step size τ_k, and newly-defined increment functions $\Delta\hat{\boldsymbol{H}}_k$ and $\Delta\hat{\boldsymbol{G}}_k$, all depend on six parameters: $\boldsymbol{A}$, $\boldsymbol{B}$, $\boldsymbol{u}$, $\boldsymbol{v}$, $\boldsymbol{b}$, and $\boldsymbol{\lambda}$ in the standard ADMM. Specifically, when addressing the NB problem of P2P energy trading using the AADMM, these six parameters must be calculated. The standard ADMM formulation for the NB problem of P2P energy trading is modeled in (SA1)-(SA8) in Supplementary Material A. The details of these six parameters, based on the formulation provided in Supplementary Material B, are given as:

$$\begin{cases}\boldsymbol{A}=\begin{bmatrix}\boldsymbol{1} & \boldsymbol{0}\\ \boldsymbol{0} & \boldsymbol{1}\end{bmatrix}\\ \boldsymbol{B}=\begin{bmatrix}\boldsymbol{1} & \boldsymbol{0}\\ \boldsymbol{0} & \boldsymbol{1}\end{bmatrix}\\ \boldsymbol{b}=[\boldsymbol{0}\quad \boldsymbol{0}]^{\mathrm{T}}\end{cases} \tag{34a}$$

$$\begin{cases}\boldsymbol{u}=[\mathbb{P}_{m,k}^{+}\quad \mathbb{P}_{n,k}^{-}]^{\mathrm{T}}\\ \boldsymbol{v}=[\hat{\mathbb{P}}_{m,k}^{+}\quad \hat{\mathbb{P}}_{n,k}^{-}]^{\mathrm{T}}\\ \boldsymbol{\lambda}_k=[\boldsymbol{\lambda}_{m,k}\quad \boldsymbol{\lambda}_{n,k}]^{\mathrm{T}}\end{cases} \tag{34b}$$

The AADMM used to solve subproblem P1 is presented in Algorithm SB1 in Supplementary Material B.

In the P2P energy trading, peers offer their electricity quantities and prices to match other trading offers. A successful transaction occurs when one peer's electricity price aligns with another peer's requirements. If this alignment does not occur, the transaction fails, prompting both peers to adjust their electricity quantities and prices. This iterative process resembles negotiation dynamics, with continuous updates and revisions to electricity offers and trading prices. The updating process is consistent with the solving methodology of ADMM. Thus, in this paper, the trading quantities and prices of electricity are determined using AADMM, ensuring the feasibility and effectiveness of the control order.

In the AADMM, the operational strategies of various DGRs in each village, power exchange with the upstream network, and energy exchange through P2P energy trading are determined and updated using model (SB4) in Supplementary Material B. Subsequently, each village sends this information to the RDNO. The RDNO then minimizes the total network loss cost and allocates it proportionally among village participants using model (SB5) in Supplementary Material B. Following this, the RDNO updates P2P energy trading prices via model (SB6) in Supplementary Material B, and the trading prices are sent to each village. If the AADMM converges, the process concludes; otherwise, it iterates. The energy trading prices, represented by the dual variable $\boldsymbol{\lambda}$, are determined by AADMM. Each iteration involves a matching process among peers, where each peer adjusts its strategies until the convergence is achieved. The successful direct energy trading between peers occur upon convergence. Once the AADMM converges, the energy trading price $\boldsymbol{\lambda}$ is finalized. The AADMM manages the trading orders based on strategy updates in each iteration to ensure the effective control. The solution post-convergence represents the optimal trading strategies for participants.

The operational strategies for various DGRs, power exchange with the upstream network, and energy exchange through P2P energy trading for each village are communicated to RDNO. In turn, the RDNO provides information on allocated network loss costs and updates on trading prices back to each village. The information of each village exchanged with the RDNO remains confidential to the respective village participants, because the RDNO acts as a virtual entity facilitating energy management via P2P energy trading. The information sent to this virtual platform is not disclosed to other peers, ensuring that each peer considers their information private. Similarly, details such as allocated network loss costs and updated trading prices sent by the RDNO to each village are treated as confidential by those villages. The RDNO only shares information relevant to each specific peer and does not distribute it to others.

For subproblem P2, the coupling variables $\hat{\pi}_m^+$ and $\hat{\pi}_n^-$ are introduced, which modifies this subproblem as:

$$\begin{cases}\max\limits_{\{\pi_m^+,\pi_n^-\}}\left\{\prod\limits_{m\in\mathbb{V}^+}(C_m^+-C_{m,\mathrm{P2P}*}^+-C_{m,\mathrm{loss}*}^+-\pi_m^+)\cdot\right.\\ \qquad\left.\prod\limits_{n\in\mathbb{V}^-}(C_n^--C_{n,\mathrm{P2P}*}^--C_{n,\mathrm{loss}*}^--\pi_n^-)\right\}\\ \text{s.t. (13), (14)}\end{cases} \tag{35a}$$

$$\pi_m^+=\hat{\pi}_m^+ \tag{35b}$$

$$\pi_n^-=\hat{\pi}_n^- \tag{35c}$$

The update of variables in P2 is not presented for the sake of conciseness, as it is like that of P1.

V. Case Study

In this section, the proposed P2P-based energy management framework is applied to an RDN consisting of 15 buses and 14 branches, as described in [48] and illustrated in Fig. 2. The AADMM is implemented in MATLAB 2018a on a desktop with an AMD Athlon™ X4 870K Quad Core Processor and 8 GB of RAM. The subproblems P1 and P2 are solved using CPLEX 12.6.2.

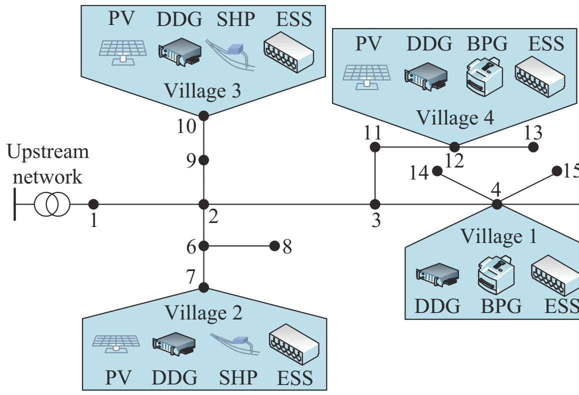

Fig. 2. Topology of studied RDN.

The voltage amplitude bounds are set to be 0.95 and 1.05 p.u.. Each transmission line has a maximum capacity of 1 MW for active power. Each bus corresponds to a village load, and four interactive villages are connected to buses 4, 7, 10, and 12. The DGRs for these four interactive villages are detailed in Supplementary Material C Table SCI. The PV outputs and load profiles for these villages based on [49] are shown in Supplementary Material C Fig. SC2.

The operational cost parameters a_2 and a_1 for DDG are 5 and 41.1, respectively. The unit operational costs for SHP and BPG are 17.6 \$/MWh and 38.3 \$/MWh, respectively. The degradation cost coefficient for ESS, assumed to be battery storage in this paper, is set to be 20 \$/MWh. The maximum energy capacity of ESS is 2 MW, with a charging/discharging efficiency of 0.95 and its SoC range of [0.1, 0.9]. Villages purchase power from the upstream network at a price from CAISO [50] and sell power to the network at half the purchasing price. The operational horizon spans 24 hours per day. The parameters for AADMM are detailed and summarized based on [51] in Supplementary Material A Table SAII.

A. Energy Exchange Results

This paper conducts two cases to validate the effectiveness of the proposed P2P-based energy management framework.

1) Case 1: a centralized energy management framework, where village participants can only exchange energy with the upstream network without engaging in P2P energy trading.

2) Case 2: the proposed P2P-based energy management framework, with village participants engaging in P2P energy trading.

Figure 3 illustrates the daily power exchange among four villages in Cases 1 and 2. Villages 1 and 4 function as buyers, while villages 2 and 3 serve as sellers in Case 2. Villages 2-4 optimize their PV power scheduling in both Cases 1 and 2. This optimization is attributed to the zero operational cost of PV, making PV be their preferred energy source. In Case 2, each village does not need to purchase power from the upstream network and can sell more surplus power back to it compared with Case 1. Consequently, the village participants have an adequate power supply to meet their demands and sell excess electricity, thereby reducing operational costs.

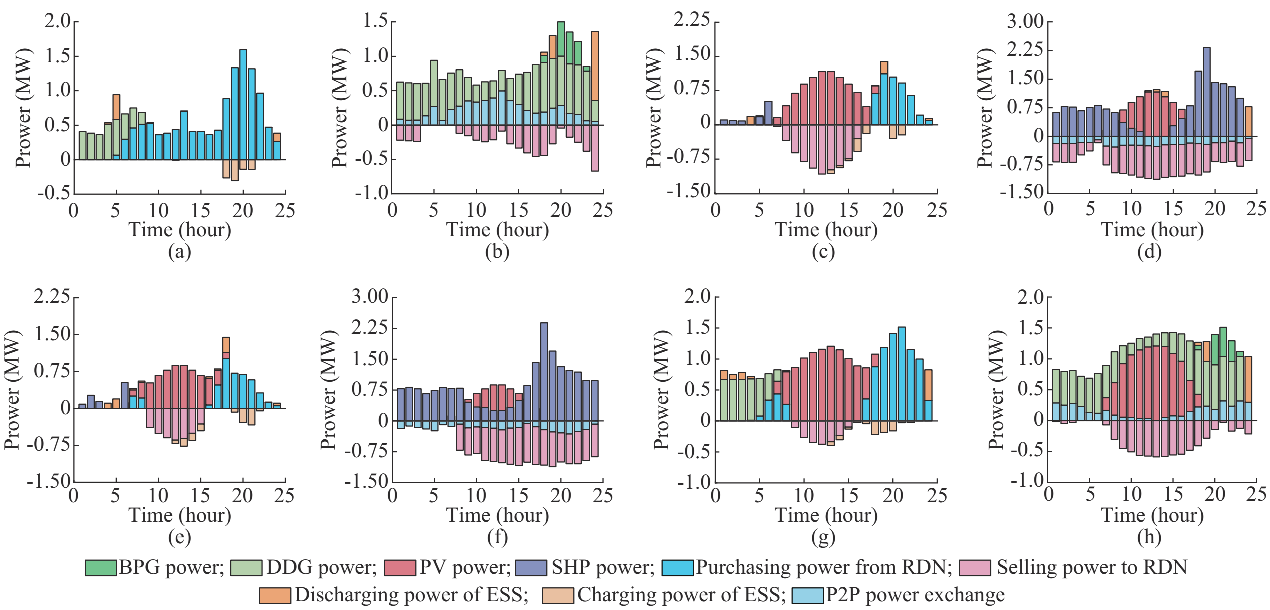

Fig. 3. Daily power exchange among four villages in Cases 1 and 2. (a) Village 1 in Case 1. (b) Village 1 in Case 2. (c) Village 2 in Case 1. (d) Village 2 in Case 2. (e) Village 3 in Case 1. (f) Village 3 in Case 2. (g) Village 4 in Case 1. (h) Village 4 in Case 2.

In both cases, the higher unit cost of DDG makes villages 1 and 4 consume more power from DDG than from BPG. Conversely, villages 2 and 3 utilize SHP due to its lower cost in comparison to DDG. The total external power supplied by the slack bus over the simulation horizon in Cases 1 and 2 is 10.66 MW and 5.56 MW, respectively. Notably, the external power supplied in Case 2 is lower than that in Case 1. Assuming that the external power reflects the energy utilization efficiency, the result indicates that the energy utilization efficiency in Case 2 is improved by 48% compared with that in Case 1.

The ESS primarily coordinates various DGRs through charging and discharging operations to minimize the operational costs and optimize the performance. The ESS significantly influences the operation of DGRs and the overall system operational costs. As shown in Fig. 3, the ESS affects the decision-making in each village in Case 1, as well as P2P energy trading in Case 2. Notably, compared with Case 2, the ESS charges and discharges during more time slots in Case 1 due to the limitation of exchanging energy solely with the upstream network. Villages utilize their ESSs to charge during periods with surplus power generation and to discharge during periods of insufficient power generation. The energy discharged from ESS reduces the need to purchase expensive energy from the upstream grid. In contrast, in Case 2, ESS discharges only during a few time slots, as the villages can directly exchange energy through P2P energy trading. Peers engage in P2P energy trading to share excess power generation for mutual benefit, eliminating the necessity to store surplus energy in ESS, thereby reducing the operational costs. Consequently, the ESS discharges only during specific time slots, serving as emergency backups to prevent power shortages.

Table I presents the operational cost, network loss cost, and payments for the four villages. The operational costs for all four villages in Case 2 are lower than those in Case 1. The total cost for all four villages is significantly reduced from \$2999.88 to \$882.64, representing a 71% reduction. Moreover, the total network loss cost decreases from \$185.52 to \$10.87. It is important to note that the total network loss cost in Case 1 is calculated using objectives (1) and (9), without considering the loss costs of individual village and P2P energy trading. This demonstrates that the proposed P2P-based energy management framework effectively reduces the total network loss cost.

TABLE I
OPERATIONAL COST, NETWORK LOSS COST, AND PAYMENTS FOR FOUR VILLAGES

Village	Case 1		Case 2		
	Operational cost (\$)	Network loss cost (\$)	Operational cost (\$)	Network loss cost (\$)	Payment (\$)
1	1185.21	-	336.07	3.19	104.01
2	395.18	-	101.77	2.80	−105.39
3	464.15	-	168.24	2.55	−102.64
4	955.34	-	276.56	2.33	106.13

B. Bus Voltage and Branch Power Flow

An essential indicator for measuring electrification levels is voltage quality. This subsection explores the impact of P2P energy trading on voltage improvement by comparing the two cases. Figure 4 illustrates the per-unit voltage values for all buses (excluding the slack bus) with different colors in both cases. In Case 1, the voltage at each bus drops significantly over the 24-hour period, with sharp decreases observed at 04:00 and increases at 18:00. In contrast, Case 2 exhibits much smoother voltage fluctuations, remaining within the range of [0.95, 0.99]p.u.. Furthermore, Fig. 5 illustrates the average voltage of UDN, calculated as the sum of voltages across all buses in each time slot divided by the total number of buses. The average voltage of UDN in Case 2 ranges from 0.975 to 0.985 p.u., indicating a smaller voltage drop compared with Case 1. This demonstrates that the direct energy exchange among village participants through P2P energy trading effectively reduces the voltage drop of both the UDN and buses, thereby enhancing the voltage quality and improving rural electrification levels.

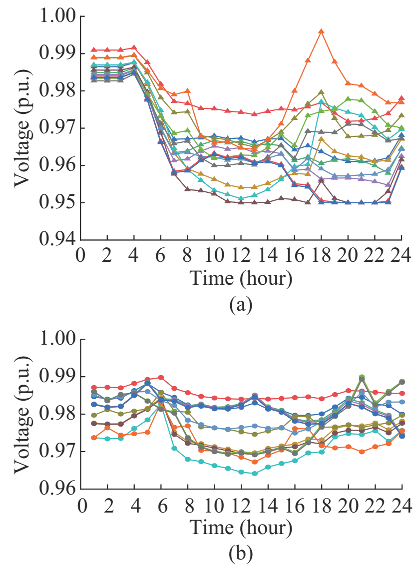

Fig. 4. Per-unit voltage values for all buses in Cases 1 and 2. (a) Case 1. (b) Case 2.

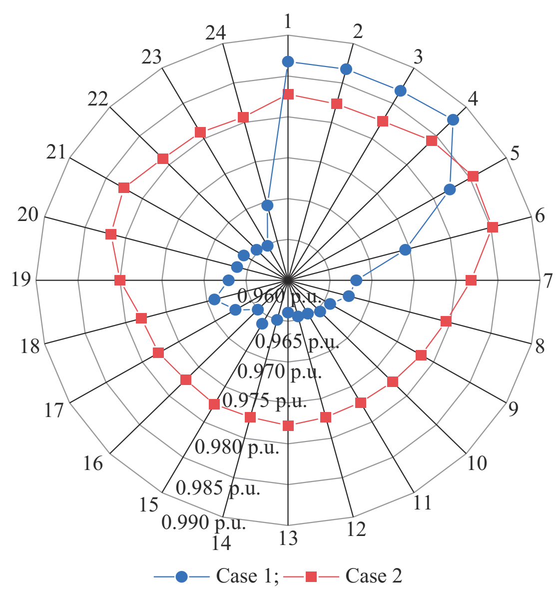

Fig. 5. Average voltage of UDN in Cases 1 and 2.

Figure 6 compares the active power flows of all branches with different colors in the two cases, while Supplementary Material C Fig. SC3 presents the comparison of reactive power flows. In both cases, the active power flow of each branch remains within the range of $[0, 1]$MW. However, in Case 1, some branches exhibit higher active power flows than those in Case 2. This indicates that the community-based villages engaging in P2P energy trading effectively reduce the power flow of branches, thereby mitigating grid congestion. If distribution lines have limited transmission capacity, such as a maximum of 0.5 MW, the congestion issues may emerge in Case 1. If the distribution lines have a limited transmission capacity, such as a maximum of 0.5 MW, the congestion issues may arise in Case 1, where the power system could rely on P2P energy trading to alleviate the line congestion.

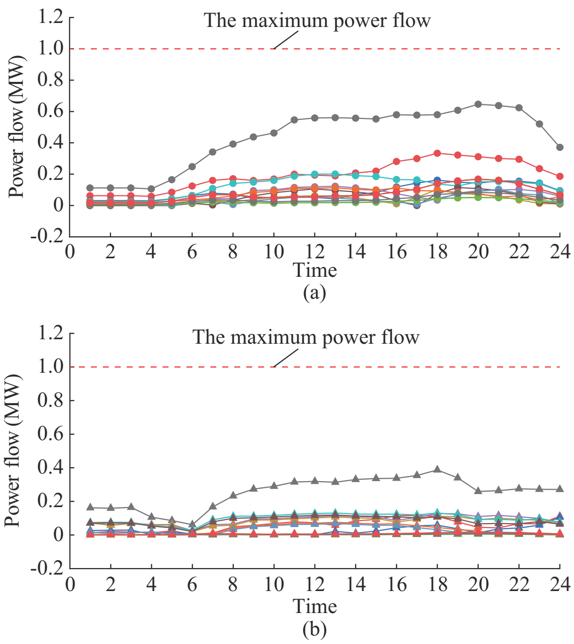

Fig. 6. Active power flows of all branches in Cases 1 and 2. (a) Case 1. (b) Case 2.

C. IEEE 33-bus and 118-bus Distribution Systems

The proposed P2P-based energy management framework is also applied to IEEE 33-bus and 118-bus distribution systems to validate its scalability, which are based on [52] and [53], respectively. The four villages are connected to buses 5, 16, 20, and 29 in the IEEE 33-bus distribution system and to buses 34, 65, 89, and 104 in the IEEE 118-bus distribution system. Various results such as energy trading volumes, operational costs, and allocated network loss costs are compared in these two systems, as presented in Supplementary Material C Tables SCIII and SCIV.

In Case 2, the operational costs for four villages connected to IEEE 33-bus distribution system are \$146.31, \$78.74, \$74.60, and \$330.70, all of which are lower than those in Case 1. Villages 1 and 4 engage in P2P energy trading, purchasing 9.49 MW and 8.90 MW of power, respectively, at costs of \$90.34 and \$85.34. Meanwhile, villages 2 and 3 sell 5.52 MW and 13.11 MW of power, earning \$74.91 and \$105.77, respectively. Additionally, the total network loss cost is \$318.02 in Case 1 and \$18.74 in Case 2, indicating that the network loss costs in Case 1 are higher than those in Case 2. Similarly, the operational costs for four villages in Case 2 of IEEE 118-bus distribution system are also lower than those in Case 1. The total network loss costs are \$65.59 and \$847.69 in Cases 2 and 1, respectively.

Additionally, the average voltages in Cases 1 and 2 are presented in Supplementary Material C Figs. SC4 and SC5, respectively. It is evident that the voltage drops in both systems in Case 2 are lower than those in Case 1. This observation implies that the proposed P2P-based energy management framework has the potential to enhance voltage quality in larger-scale distribution systems, thereby enhancing the overall electrification level of systems. Furthermore, the proposed P2P-based energy management framework is scalable to larger distribution systems.

D. Convergence and Computational Performance

Figures 7-9 illustrate the convergence performance of standard ADMM and AADMM in solving problem P1. The stopping tolerance ε^{tol} in the AADMM is set to be 10^{-3}. Overall, the rates of decrease in both primal and dual residuals are faster with AADMM compared with standard ADMM. Figure 9 presents the relative residual, i.e., (21), demonstrating that AADMM and standard ADMM converge in 134 and 1086 iterations, respectively. This indicates an 86% improvement in convergence speed with AADMM. Upon convergence, the primal residual r_k and dual residual d_k are 6×10^{-4} and 8×10^{-2}, respectively. Although the dual residual is below the stopping tolerance, the relative residual is 7×10^{-4}, which satisfies the convergence condition. Therefore, the AADMM demonstrates a superior convergence performance compared with the standard ADMM.

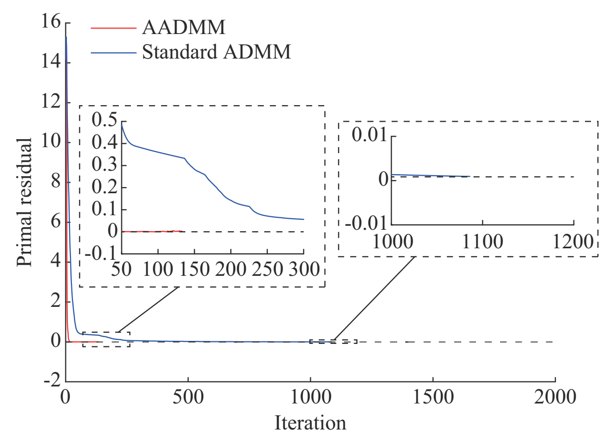

Fig. 7. Primal residual of AADMM and standard ADMM.

Due to the adaptive nature of AADMM, it can be initialized with random values for τ_0. We investigate the sensitivity of different initial penalty parameters and the sensitivity analysis results are given in Table II. Notably, the standard ADMM fails to converge within the maximum number of iterations (denoted as $k_{\max}=2000$, as illustrated in Supplementary Material C Table SCII) when $\tau_0=0.1$. Furthermore, the AADMM exhibits the fastest convergence during sensitivity testing when $\tau_0=1$. Hence, initializing the penalty parameter closer to 1 is recommended.

The convergence iterations for standard ADMM with different initial penalty parameters exhibit notable differences. In contrast, no such distinctions are observed in the sensitivity results for AADMM. This indicates that the standard AD-

MM is highly sensitive to the choice of the initial penalty parameter, making its convergence performance largely dependent on this setting. Conversely, the AADMM demonstrates stability irrespective of the initial value.

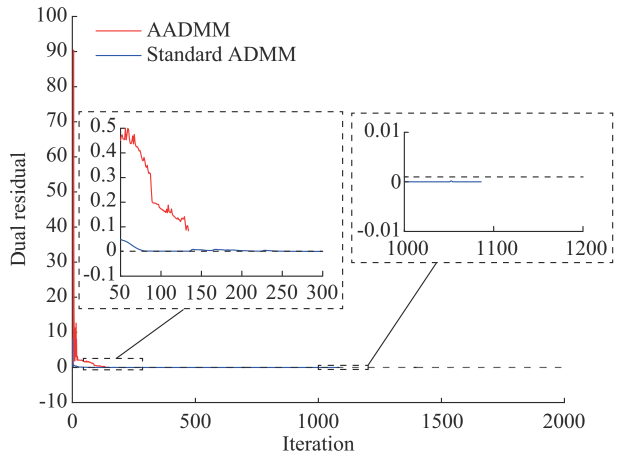

Fig. 8. Dual residual of AADMM and standard ADMM.

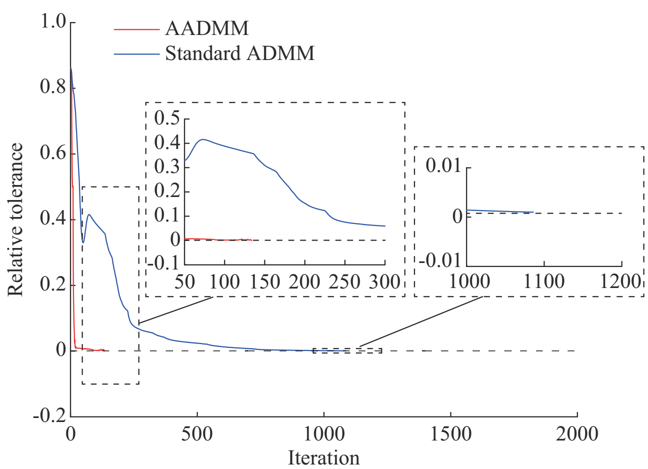

Fig. 9. Relative residual of AADMM and standard ADMM.

TABLE II
CONVERGENCE RESULTS WITH DIFFERENT INITIAL PENALTY PARAMETERS

Method	k		
	$\tau_0=0.1$	$\tau_0=1$	$\tau_0=5$
AADMM	182	134	162
Standard ADMM	2000*	1086	244

Note: * represents that the standard ADMM fails to converge after 2000 iterations.

This study adopts a hybrid step size rule based on [42], as formulated in (31), to estimate curvatures α and β. While some studies have proposed other step size rules for the adaptive penalty parameter in ADMM such as the BB1 and BB2 rules in [39], and the RB rule in [38] inspired by the BB method, they may exhibit potential instability in their algorithmic characteristics. Such instability can hinder the convergence speed when solving certain optimization problems or increase computational time. To demonstrate the advantages of the hybrid step size rule, we conduct a comparative analysis of performance using these different step size rules. The initial penalty parameter is uniformly set to be $\tau_0=1$ for all methods that employ different step size rules. Table III and Fig. 10 present the number of iterations until convergence and the relative residuals of different methods with various step size rules, respectively.

TABLE III
NUMBER OF ITERATIONS OF DIFFERENT METHODS ADOPTING VARIOUS STEP SIZE RULES

Method	Number of iterations
Standard ADMM	1086
AADMM	134
ADMM-BB1 in [39]	261
ADMM-BB2 in [39]	418
ADMM-RB in [38]	699

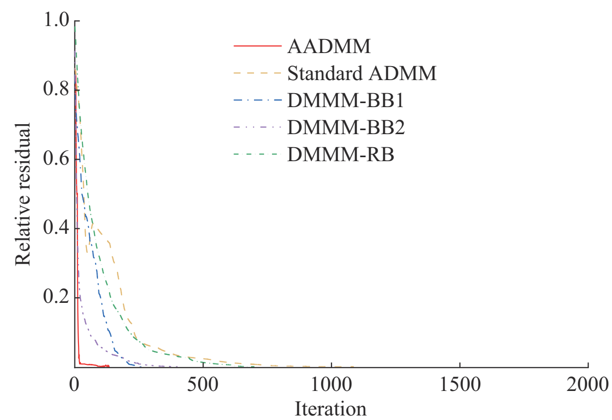

Fig. 10. Relative residual of different methods with various step size rules.

The four step size rules for the adaptive penalty parameter effectively reduce the number of iterations. In this paper, the hybrid step size rule in AADMM achieves the fastest convergence compared with other step size rules, requiring only 134 iterations and demonstrating a rapid decrease in relative residuals.

VI. CONCLUSION

This paper proposes a P2P-based energy management framework for a remote RDN. This framework enables villages to integrate multiple DGRs and directly exchange energy with each other, thereby reducing operational costs. The P2P energy trading is formulated as an NB problem, which is further decomposed into two subproblems. To solve these subproblems, an improved ADMM-based distributed optimization method, i.e., AADMM, is proposed. The AADMM, inspired by the BB method and gradient descent, employs curvature estimation to automatically adjust the penalty parameter. Simulation results demonstrate the advantages of the proposed P2P-based energy management framework and the improved convergence performance of AADMM. Compared with the centralized energy management framework, the proposed P2P-based energy management framework reduces the operational costs of villages and enhances the energy utilization efficiency through direct energy exchange. Additionally, the convergence speed of AADMM is improved by 88% compared with the standard ADMM.

The proposed P2P-based energy management framework enhances the rural electrification through three key aspects: market mechanisms, voltage quality improvement, and branch power flow optimization. First, it leverages market mechanisms to optimize the utilization of DGRs, challenging the traditional centralized energy trading framework. This diversification of energy trading patterns in rural areas provides alternative solutions for rural community energy trading. Second, this framework effectively mitigates voltage drops and fluctuations, leading to improved voltage quality, thereby contributing to enhanced rural electrification through superior voltage regulation. Lastly, the P2P energy trading reduces power flow on transmission lines, ensuring the safe system operation within established capacity limits.

Future research will primarily explore the interactions between multiple energy sources within RDN, with a focus on integrated electricity-gas and electricity-heat systems.

References

[1] S. Kanwal, B. Khan, and M. Q. Rauf, "Infrastructure of sustainable energy development in Pakistan: a review," *Journal of Modern Power Systems and Clean Energy*, vol. 8, no. 2, pp. 206-218, Mar. 2020.

[2] The World Bank. (2022, Dec.). Urban development. [Online]. Available: https://www.worldbank.org/en/topic/urbandevelopment/overview.

[3] A. Shahsavari and M. Akbari, "Potential of solar energy in developing countries for reducing energy-related emissions," *Renewable and Sustainable Energy Reviews*, vol. 90, pp. 275-291, Jul. 2018.

[4] V. Vai, M. C. A. Herault, B. Raison *et al*., "Optimal low-voltage distribution topology with integration of PV and storage for rural electrification in developing countries: a case study of Cambodia," *Journal of Modern Power Systems and Clean Energy*, vol. 8, no. 3, pp. 531-539, May 2020.

[5] S. C. Bhattacharyya and S. Ohiare, "The Chinese electricity access model for rural electrification: approach, experience and lessons for others," *Energy Policy*, vol. 49, pp. 676-687, Oct. 2012.

[6] F. Almeshqab and T. S. Ustun, "Lessons learned from rural electrification initiatives in developing countries: insights for technical, social, financial and public policy aspects," *Renewable and Sustainable Energy Reviews*, vol. 102, pp. 35-53, Mar. 2019.

[7] F. O. Omole, O. K. Olajiga, and T. M. Olatunde, "Challenges and successes in rural electrification: a review of global policies and case studies," *Engineering Science & Technology Journal*, vol. 5, no. 3, pp. 1031-1046, Mar. 2024.

[8] N. J. Williams, P. Jaramillo, J. Taneja *et al*., "Enabling private sector investment in microgrid-based rural electrification in developing countries: a review," *Renewable and Sustainable Energy Reviews*, vol. 52, pp. 1268-1281, Dec. 2015.

[9] X. Liang and M. Abbasipour, "HVDC transmission and its potential application in remote communities: current practice and future trend," *IEEE Transactions on Industry Applications*, vol. 58, no. 2, pp. 1706-1719, Mar. 2022.

[10] C. Milchram, R. Künneke, N. Doorn *et al*., "Designing for justice in electricity systems: a comparison of smart grid experiments in the Netherlands," *Energy Policy*, vol. 147, p. 111720, Dec. 2020.

[11] C. I. Ciontea and F. Iov, "A study of load imbalance influence on power quality assessment for distribution networks," *Electricity*, vol. 2, no. 1, pp. 77-90, Mar. 2021.

[12] G. Falchetta, S. Pachauri, S. Parkinson *et al*., "A high-resolution gridded dataset to assess electrification in sub-Saharan Africa," *Scientific Data*, vol. 6, p. 110, Jul. 2019.

[13] L. Moretti, M. Astolfi, C. Vergara *et al*., "A design and dispatch optimization algorithm based on mixed integer linear programming for rural electrification," *Applied Energy*, vol. 233-234, pp. 1104-1121, Jan. 2019.

[14] H. Tan, W. Yan, Z. Ren *et al*., "Distributionally robust operation for integrated rural energy systems with broiler houses," *Energy*, vol. 254, p. 124398, Sept. 2022.

[15] Y. Wang, L. Guo, Y. Ma *et al*., "Study on operation optimization of decentralized integrated energy system in northern rural areas based on multi-objective," *Energy Reports*, vol. 8, pp. 3063-3084, Nov. 2022.

[16] K. Murugaperumal, S. Srinivasn, and G. R. K. D. S. Prasad, "Optimum design of hybrid renewable energy system through load forecasting and different operating strategies for rural electrification," *Sustainable Energy Technologies and Assessments*, vol. 37, p. 100613, Feb. 2020.

[17] Y. Liu, Y. Gao, Y. Li *et al*., "A non-iterative network utilization pricing mechanism for P2P energy trading," *CSEE Journal of Power and Energy Systems*, vol. 10, no. 3, pp. 1301-1306, May 2024.

[18] J. Yang, W. Xu, K. Ma *et al*., "A three-stage multi-energy trading strategy based on P2P trading mode," *IEEE Transactions on Sustainable Energy*, vol. 14, no. 1, pp. 233-241, Jan. 2023.

[19] M. I. Azim, G. Lankeshwara, W. Tushar *et al*., "Dynamic operating envelope-enabled P2P trading to maximize financial returns of prosumers," *IEEE Transactions on Smart Grid*, vol. 15, no. 2, pp. 1978-1990, Mar. 2024.

[20] J. Guerrero, A. C. Chapman, and G. Verbič, "Decentralized P2P energy trading under network constraints in a low-voltage network," *IEEE Transactions on Smart Grid*, vol. 10, no. 5, pp. 5163-5173, Sept. 2019.

[21] H. Sheng, C. Wang, X. Dong *et al*., "Incorporating P2P trading into DSO's decision-making: a DSO-prosumers cooperated scheduling framework for transactive distribution system," *IEEE Transactions on Power Systems*, vol. 38, no. 3, pp. 2362-2375, May 2023.

[22] T. Morstyn, A. Teytelboym, C. Hepburn *et al*., "Integrating P2P energy trading with probabilistic distribution locational marginal pricing," *IEEE Transactions on Smart Grid*, vol. 11, no. 4, pp. 3095-3106, Jul. 2020.

[23] M. Yan, M. Shahidehpour, A. Paaso *et al*., "Distribution network-constrained optimization of peer-to-peer transactive energy trading among multi-microgrids," *IEEE Transactions on Smart Grid*, vol. 12, no. 2, pp. 1033-1047, Mar. 2021.

[24] H. Nezamabadi and V. Vahidinasab, "Arbitrage strategy of renewable-based microgrids via peer-to-peer energy-trading," *IEEE Transactions on Sustainable Energy*, vol. 12, no. 2, pp. 1372-1382, Apr. 2021.

[25] C. Liu and Z. Li, "Comparison of centralized and peer-to-peer decentralized market designs for community markets," *IEEE Transactions on Industry Applications*, vol. 58, no. 1, pp. 67-77, Jan. 2022.

[26] Q. Li, Y. Liao, K. Wu *et al*., "Parallel and distributed optimization method with constraint decomposition for energy management of microgrids," *IEEE Transactions on Smart Grid*, vol. 12, no. 6, pp. 4627-4640, Nov. 2021.

[27] D. K. Molzahn, F. Dörfler, H. Sandberg *et al*., "A survey of distributed optimization and control algorithms for electric power systems," *IEEE Transactions on Smart Grid*, vol. 8, no. 6, pp. 2941-2962, Nov. 2017.

[28] X. Le, S. Chen, Z. Yan *et al*., "Enabling a transactive distribution system via real-time distributed optimization," *IEEE Transactions on Smart Grid*, vol. 10, no. 5, pp. 4907-4917, Sept. 2019.

[29] H. Wang and J. Huang, "Incentivizing energy trading for interconnected microgrids," *IEEE Transactions on Smart Grid*, vol. 9, no. 4, pp. 2647-2657, Jul. 2018.

[30] H. Kim, J. Lee, S. Bahrami *et al*., "Direct energy trading of microgrids in distribution energy market," *IEEE Transactions on Power Systems*, vol. 35, no. 1, pp. 639-651, Jan. 2020.

[31] X. He, Y. Zhao, and T. Huang, "Optimizing the dynamic economic dispatch problem by the distributed consensus-based ADMM approach," *IEEE Transactions on Industrial Informatics*, vol. 16, no. 5, pp. 3210-3221, May 2020.

[32] Z. Guo, P. Pinson, S. Chen *et al*., "Online optimization for real-time peer-to-peer electricity market mechanisms," *IEEE Transactions on Smart Grid*, vol. 12, no. 5, pp. 4151-4163, Sept. 2021.

[33] Z. Lu, L. Bai, J. Wang *et al*., "Peer-to-peer joint electricity and carbon trading based on carbon-aware distribution locational marginal pricing," *IEEE Transactions on Power Systems*, vol. 38, no. 1, pp. 835-852, Jan. 2023.

[34] C. Chen, Y. Li, W. Qiu *et al*., "Cooperative-game-based day-ahead scheduling of local integrated energy systems with shared energy storage," *IEEE Transactions on Sustainable Energy*, vol. 13, no. 4, pp. 1994-2011, Oct. 2022.

[35] C. Song, S. Yoon, and V. Pavlovic, "Fast ADMM algorithm for distributed optimization with adaptive penalty," *Proceedings of the AAAI Conference on Artificial Intelligence*, vol. 30, no. 1, pp. 1-11, Feb. 2016.

[36] T. Goldstein, M. Li, and X. Yuan, "Adaptive primal-dual splitting methods for statistical learning and image processing," *Advances in Neural Information Processing Systems*, vol. 28, pp. 2089-2097, Dec.

2015.
[37] E. Ghadimi, A. Teixeira, I. Shames *et al*., "On the optimal step-size selection for the alternating direction method of multipliers," *IFAC Proceedings Volumes*, vol. 45, no. 26, pp. 139-144, Sept. 2012.
[38] B. He, H. Yang, and S. Wang, "Alternating direction method with self-adaptive penalty parameters for monotone variational inequalities," *Journal of Optimization Theory and Applications*, vol. 106, no. 2, pp. 337-356, Jan. 2000.
[39] S. Crisci, V. de Simone, and M. Viola, "On the adaptive penalty parameter selection in ADMM," *Algorithms*, vol. 16, no. 6, p. 264, May 2023.
[40] B. Gao, Y. Zhu, Y. Li *et al*., "Optimal operation strategy analysis with scenario generation method based on principal component analysis, density canopy, and *K*-medoids for integrated energy systems," *Journal of Modern Power Systems and Clean Energy*, vol. 12, no. 1, pp. 89-100, Jan. 2024.
[41] B. Sun, R. Jing, L. Ge *et al*., "Quick hosting capacity evaluation based on distributed dispatching for smart distribution network planning with distributed generation," *Journal of Modern Power Systems and Clean Energy*, vol. 12, no. 1, pp. 128-140, Jan. 2024.
[42] Z. Xu, M. A. T. Figueiredo, and T. Goldstein, "Adaptive ADMM with spectral penalty parameter selection," *Proceedings of the 20th International Conference on Artificial Intelligence and Statistics*, Fort Lauderdale, USA, Apr. 2017, pp. 718-727.
[43] J. Barzilai and J. M. Borwein, "Two-point step size gradient methods," *IMA Journal of Numerical Analysis*, vol. 8, no. 1, pp. 141-148, Jan. 1988.
[44] C. Cartis, N. I. M. Gould, and P. L. Toint, "On the complexity of steepest descent, Newton's and regularized Newton's methods for nonconvex unconstrained optimization problems," *SIAM Journal on Optimization*, vol. 20, no. 6, pp. 2833-2852, Jan. 2010.
[45] J. Eckstein and D. P. Bertsekas, "On the Douglas-Rachford splitting method and the proximal point algorithm for maximal monotone operators," *Mathematical Programming*, vol. 55, no. 1, pp. 293-318, Apr. 1992.
[46] R. Rockafellar, *Convex Analysis*. Princeton: Princeton University Press, 1970.
[47] B. Zhou, L. Gao, and Y. Dai, "Gradient methods with adaptive step-sizes," *Computational Optimization and Applications*, vol. 35, no. 1, pp. 69-86, Mar. 2006.
[48] D. Das, D. P. Kothari, and A. Kalam, "Simple and efficient method for load flow solution of radial distribution networks," *International Journal of Electrical Power & Energy Systems*, vol. 17, no. 5, pp. 335-346, Oct. 1995.
[49] G. J. Prinsloo, "Scoping exercise to determine load profile archetype reference shapes for solar co-generation models in isolated off-grid rural African Villages," *Journal of Energy in Southern Africa*, vol. 27, no. 3, p. 11, Nov. 2016.
[50] W. Shi, X. Xie, C. Chu *et al*., "Distributed optimal energy management in microgrids," *IEEE Transactions on Smart Grid*, vol. 6, no. 3, pp. 1137-1146, May 2015.
[51] Z. Xu, "Alternating optimization: constrained problems, adversarial networks, and robust models," M.S. thesis, University of Maryland, College Park, USA, 2019.
[52] M. E. Baran and F. Wu, "Network reconfiguration in distribution systems for loss reduction and load balancing," *IEEE Transactions on Power Delivery*, vol. 4, no. 2, pp. 1401-1407, Apr. 1989.
[53] D. Zhang, Z. Fu, and L. Zhang, "An improved TS algorithm for loss-minimum reconfiguration in large-scale distribution systems," *Electric Power Systems Research*, vol. 77, no. 5-6, pp. 685-694, Apr. 2007.

Yi Liu received the B.S. degree from Zhengzhou University of Light Industry, Zhengzhou, China, in 2018, and the M.S. degree from China Three Gorges University, Yichang, China, in 2021. He is currently pursuing the Ph.D. degree in Sichuan University, Chengdu, China. His research interests include planning, operation, and market of rural energy system.

Xiao Xu received the B.S. degree from Qingdao University of Technology, Qingdao, China, in 2017, and the Ph.D. degree from University of Electronic Science and Technology of China, Chengdu, China, in 2021. He is currently working as an Associate Professor in Sichuan University, Chengdu, China. His research interests include operation optimization of energy system.

Chuanjiang Deng received the M.S. degree from University of Electronic Science and Technology of China, Chengdu, China, in 2012. He is currently a Senior Engineer at the Aba Power Supply Company of State Grid Sichuan Electric Power Company, Abazhou Autonomous Prefecture, China. His research interests include power construction, transformation, and distribution engineering.

Junyong Liu received the B.S. and M.S. degrees from Sichuan University, Chengdu, China, in 1984 and 1989, respectively, and the Ph.D. degree from Brunel University, London, UK, in 1998. He is currently working as a Professor in Sichuan University. His research interests include smart energy, ecological agriculture, and electricity market.

Lixiong Xu received the B.S., M.S., and Ph.D. degrees from Sichuan University, Chengdu, China, in 2003, 2006, and 2014, respectively. He is currently working as an Associate Professor in Sichuan University. His research interests include smart grid, power system security, and stability.

Youbo Liu received the B.S., M.S., and Ph.D. degrees from Sichuan University, Chengdu, China, in 2005, 2008, and 2011, respectively. He is currently working as a Professor in Sichuan University. His research interests include active distribution network and low-carbon electricity market.

Nan Yang received the B.S. degree from Taiyuan University of Technology, Taiyuan, China, in 2009, and the Ph.D. degree from Wuhan University, Wuhan, China, in 2014. He is currently working as a Professor in China Three Gorges University, Yichang, China. His research interests include power system operation and planning.

Yichen Luo received the B.S. degree from Northeast Electric Power University, Jilin, China, in 2018, and the M.S. degree from Guangxi University, Nanning, China, in 2022. She is currently pursuing the Ph.D. degree in Sichuan University, Chengdu, China. Her research interests include security analysis and defense methods of cyber-physical power system.

Shafqat Jawad is currently pursuing the Ph.D. degree in electrical engineering with the College of Electrical Engineering, Sichuan University, Chengdu, China. His research interests include electric vehicle, planning and operation of interdependent power and transportation network, and distributed energy source.